

UNCLASSIFIED

AD

408 664

DEFENSE DOCUMENTATION CENTER

FOR

SCIENTIFIC AND TECHNICAL INFORMATION

CAMERON STATION, ALEXANDRIA, VIRGINIA



UNCLASSIFIED

NOTICE: When government or other drawings, specifications or other data are used for any purpose other than in connection with a definitely related government procurement operation, the U. S. Government thereby incurs no responsibility, nor any obligation whatsoever; and the fact that the Government may have formulated, furnished, or in any way supplied the said drawings, specifications, or other data is not to be regarded by implication or otherwise as in any manner licensing the holder or any other person or corporation, or conveying any rights or permission to manufacture, use or sell any patented invention that may in any way be related thereto.

6342

AFCRL-63-120(A)

408 664

CATALOGED BY DDC
AS AD No. 408 664

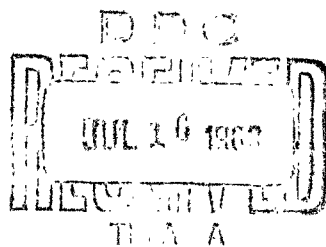
SEMICONDUCTOR DEVICE CONCEPTS

General Electric Company
General Electric Research Laboratory
Schenectady, New York

Scientific Report No. 3A
AF 19(628)-329
February 28, 1963
Project 4608
Task 460804

Prepared for

AIR FORCE CAMBRIDGE RESEARCH LABORATORIES
OFFICE OF AEROSPACE RESEARCH
UNITED STATES AIR FORCE
BEDFORD, MASSACHUSETTS



Requests for additional copies by Agencies of the Department of Defense, their contractors, and other Government agencies should be directed to the:

DEFENSE DOCUMENTATION CENTER (DDC)
ARLINGTON HALL STATION
ARLINGTON 12, VIRGINIA

Department of Defense contractors must be established for ASTIA services or have their "need-to-know" certified by the cognizant military agency of their project or contract.

All other persons and organizations should apply to the:

U. S. DEPARTMENT OF COMMERCE
OFFICE OF TECHNICAL SERVICES
WASHINGTON 25, D. C.

TABLE OF CONTENTS

	<u>Page</u>
Abstract	3
A. Electrical Measurements on CdS	5
B. Measurement of the Cd-CdS Liquidus	8
Introduction	8
Procedure	8
Results	10
Discussion	10
Acknowledgements	13
References	14
Figure Captions	15
Figures	16
C. A Double Acceptor Defect in CdTe	18
References	23
Figure Captions	24
Figures	25
D. Donor and Acceptor Centers in Al-Doped ZnSe	27
Introduction	27
Experimental Techniques and Results	27
Material Preparation	27
Steady State Hall Measurements	29
Photo-Hall Measurements	31
Discussion	34
Shallow Donors	34
Double Acceptor States	36
Luminescence Centers	39
Conclusion	40
Acknowledgement	41
References	42
Figure Captions	43
Figures	44
E. Radiation From GaSb and GaAs _x P _{1-x} Junctions	49
F. Analysis of the Band-to-Band Model for the Junction	
Laser	51
Definitions	51
Assumptions	52
Analysis	54
References	58
Figure Captions	59
Figures	60
Contributors	62
Papers Sponsored Under Contract	62

Abstract

A brief review of the work on CdS performed under this contract is given with the principle conclusions to date.

The Cd-CdS liquidus has been measured between 700° and 1250°C. In the low-temperature region, the liquidus rises exponentially with temperature similar to that observed in III-V semiconducting compound systems.

A new electrically active defect center, believed to be a native double acceptor, has been observed in CdS. It shows identical behavior to a center concurrently observed in CdTe in this laboratory. These centers are formed during heat treatment in a Cd atmosphere. The centers are similar to the double acceptor centers observed in Ge in that they become very effective hole traps at low temperatures.

Al can be diffused into ZnSe crystals from liquid Zn-Al alloys. The approximate diffusion coefficient for this process at 1050°C is $2 \times 10^{-9} \text{ cm}^2/\text{sec}$. Hall measurements on ZnSe:Al have shown that the crystals contain hydrogenic donor states 0.023 eV below the conduction band edge. The crystals also exhibit the presence of double acceptor states having the ionization energy of approximately 0.11 eV. Besides these species, the ZnSe:Al crystals contain Zn vacancies which are believed to act as the major compensating species in n-type crystals, and yellow luminescence centers believed to be due to the simultaneous presence in the crystals of Al and of Zn vacancies.

Abstract (Contd.)

Studies of diffused junctions prepared from GaSb and GaAs_xP_{1-x} are continuing. Efforts to produce coherent light emission have thus far been unsuccessful.

A theoretical analysis of the threshold current density and carrier distribution in junction lasers has been carried out. Quantitative results have been obtained in terms of experimentally observable parameters. The calculated threshold current densities are reasonably close to those observed experimentally, using parameters appropriate for free electrons and holes in GaAs.

A. ELECTRICAL MEASUREMENTS ON CdS (H. H. Woodbury)

It is becoming more evident that a better understanding of how to prepare and control II-VI compounds in both p- and n-type conductivity forms is dependent on an understanding of the behavior of the native defects. This appears to be particularly true of CdS where only n-type material has been prepared. Attempts to produce p-type material by heavy doping of Cu, Ag, or Au have failed as the uncompensated acceptor impurities precipitate.¹ Direct firing in sulfur is also unsuccessful as the samples appear to always compensate on a level about 1 ev below the conduction band.¹ It has been observed that firing undoped samples at 1000°C in S (100 Atm) produce microscopically visible inhomogeneities. It is not known whether these inhomogeneities are voids (coagulation of vacancies), precipitation of excess S, or modified regions of CdS. It does seem evident that firing at higher temperatures and pressures in sulfur are of little value unless rapid quenching techniques with small samples are employed. The samples were typically 1 x 1 x 5 mm³ and were sealed in 2 mm I.D. by 8 mm O.D. quartz tubing. These ampoules were quenched by dropping from the furnace into ethylene glycol.

Because of the above failures and the apparent fruitlessness of the semiempirical approach mentioned above in producing p-type CdS, n-type CdS has been studied with the object of learning more about the native defects and how they interact (compensate) the chemical donors and acceptors. To create the basic ground work for these studies, the Cd-CdS liquidus has been measured. This work which is described in

Section B of this report has been completed and has been accepted for publication in the "Journal of the Physics and Chemistry of Solids."

A surprising result has been observed in the electrical properties of CdS fired in Cd. This is the appearance of a double acceptor center which is contrary to the idea that Cd firing should only create donors or annihilate acceptors. The observance of this center in both CdS and CdTe has been reported in a Letter entitled "A Double Acceptor Defect in CdTe" by M. R. Lorenz and H. H. Woodbury, published in "Physical Review Letters," 10, 215 (1963). This work is described below in Section C. Study of this center in CdS is being pursued. Although it is premature to identify the center, the simplest explanation is that it is a sulfur vacancy. The way in which a sulfur vacancy can act as a double acceptor is easily seen if one postulates covalent bonding in CdS. The situation then becomes analogous to the vacancy found in silicon where the four atoms surrounding the single lattice vacancy are pictured as pairing, each pair forming a bond with two anti-parallel electrons.² In the case of a sulfur vacancy in CdS, two additional electrons would be required to form such bonds between the four Cd atoms surrounding the vacancy; hence, the defect would act like a double acceptor. This would not preclude the possibility that the center could act as a donor also. However, the donor level (or levels) would have to lie below the acceptor levels.

REFERENCES

1. M. Aven and H. H. Woodbury, Final Report, Contract No. AF19(604)-8512 AFCRL-62-557 (June, 1962).
2. G. D. Watkins, J. Phys. Soc. Japan, to be published (Kyoto International Conference on Crystal and Lattice Defects).

B. MEASUREMENT OF THE Cd-CdS LIQUIDUS (H. H. Woodbury)

INTRODUCTION

It is well known that deviations from stoichiometry of the II-VI compound semiconductors can profoundly change their electrical and optical properties. However, the details of what happens when such a semiconductor is fired in one of its components are little understood. One effect on certain impurities has been shown, namely, the firing of such semiconductors in the metal component will remove or getter Cu and Ag.¹ To establish the basic ground work for such studies in CdS, a portion of the Cd-CdS liquidus has been determined. An attempt was made to determine the S-CdS liquidus but the solubility of CdS in sulfur in the temperature range accessible (up to 1000°C) was found to be very small. Only one point on the S-CdS liquidus was determined (see Fig. 1).

PROCEDURE

A weight-loss procedure was employed as follows: Single crystal pieces of high-purity CdS, ranging between 10 mg and 250 mg, were sealed in quartz tubing with 0.1 g to 1 g of Cd. For temperatures up to 1100°C, 5 mm I.D. x 7.4 mm O.D. tubing was used; at 1150°C, 4 mm I.D. x 6 mm O.D. tubing was used; and at the highest temperatures (1200°C - 1250°C), capillary tubing with 2 mm to 3 mm I.D. and 10 mm O.D. was used. The maximum temperature was limited by the softening and expansion of the quartz under the Cd pressure. Quartz tubing or rods were often placed inside the firing tubes which would hold the sample at one end of the tube (the bottom when firing) but would permit the Cd to separate upon inversion of the tube. This separation was necessary to prevent the

freezing Cd from cracking the sample. Above 900°C, the liquid Cd would become very viscous (presumably due to the dissolved sulfur) and it was necessary to mechanically tap the tube to separate the liquid from the crystal. The Cd sticking to the samples or partly embedding them was removed in cold (<10°C) dilute (7%) HNO₃. Although this treatment would apparently reduce the dissolved CdS to free sulfur, it did not measurably attack the single crystal CdS. The weight loss of the sample could thus be determined and from the known Cd metal originally in the firing tube, the Cd-CdS liquidus could be calculated. The weight loss measurements were checked for a few samples by analyzing the sulfur which had dissolved in the Cd, using standard chemical techniques. The two methods were in agreement within 10%, the reproducibility of the measurements.

The main problem encountered in the procedure was the establishment of equilibrium during the firing. It was necessary to keep the bottom end of the 2 cm to 3 cm long quartz tubes colder than the top; otherwise Cd would condense in the top. Too great a temperature gradient and worse, too great a temperature cycling, would cause material transport away from the crystal. Small crystals, separate from the original crystal, have been observed to grow under conditions of large temperature variations. For the liquidus measurements, the temperature gradient and cycling were kept less than 1°C. Different samples were fired for different lengths of time at each temperature to ensure that equilibrium was obtained. For example, reproducible results were obtained when the firing time was varied from 1/2 hour to 4 hours at the highest temperatures (1250°C) and 16 hours to 60 hours at the lowest temperatures

(700°C).

The procedure for sulfur firing was somewhat simpler since it was not necessary to separate the liquid sulfur from the samples. Also, the sulfur was easily removed from the crystals by washing them in CS_2 . The maximum temperature of the sulfur firing was limited to 1000°C, above which temperature the 2 mm I.D. x 10 mm O.D. quartz tubing would explode.

RESULTS

The averages of the calculated composition values for several runs at each of the temperatures indicated are plotted in Figs. 1 and 2. Figure 1 gives the Cd-CdS liquidus on a linear temperature-composition phase diagram. The maximum melting point, $T_m = 1475 \pm 15^\circ\text{C}$, is the value given by Addamiano.² The dashed extrapolated portion was arbitrarily drawn. Figure 2 gives the same data on a dimensionless plot.

DISCUSSION

Thermodynamic considerations give the relationship between the composition variables and the temperature provided one has a model for the equilibrium reaction. The usual first assumption is an unionized, dissociated state for the liquid. That is, the solid $(\text{AB})_s$ is assumed to melt in a liquid of composition $(1-x)\text{A}_\ell + x\text{B}_\ell$ where x is the mole fraction of the B_ℓ component in the liquid. As a first approximation, the liquid is assumed to be ideal with respect to the two, noninteracting components, A_ℓ and B_ℓ . Equating the chemical potential of the compound in the solid state to its components in the liquid state and assuming the heat of fusion to be temperature independent, one easily derives the following relationship between the melting temperature, T , and the

liquid composition, x :

$$\left(\frac{T_m}{T} - 1\right) = \left(-\frac{R}{\Delta S}\right) [\ln 4x(1-x)]. \quad (1)$$

Here T_m is the maximum melting temperature of the compound and ΔS is the entropy of fusion. The data for CdS is plotted as open circles in Fig. 2 using $\ln[4x(1-x)]$ as the ordinate. Second approximations to (1) have been derived assuming only that the solution is regular.⁽³⁾ It is noted that equation (1) still applies if the two components are assumed to be completely ionized.

It has been observed that the vapor pressure over the melt of CdS is very low compared to the vapor pressure over either component at the same temperature.² This is an indication of considerable interaction between the components in the liquid state and suggests that an undissociated model for the liquid state may be a better approximation. Specifically, assume the liquid to have excess A over B and to take the form $(1-y)A_{\lambda} + y(AB)_{\lambda}$ where y is the mole fraction of the $(AB)_{\lambda}$ component. Again, assume ideal behavior of the two components of the liquid, A_{λ} and $(AB)_{\lambda}$, and that the heat of fusion is temperature independent. One then derives the following relation for the melting temperature, T , for the equilibrium $(AB)_s \rightleftharpoons (AB)_{\lambda}$:

$$\left(\frac{T_m}{T} - 1\right) = -\frac{R}{\Delta S} \ln(y),$$

or, in terms of the variable x used in (1),

$$\left(\frac{T_m}{T} - 1\right) = -\frac{R}{\Delta S} \ln(2x), \quad x \leq 1/2. \quad (2)$$

The data for CdS is plotted as closed circles in Fig. 2 using $\ln(2x)$ as the ordinate. It is evident that plotted this way, the data better approximates the ideal behavior of a straight line drawn through the maximum melting point, $(\frac{T_m}{T} - 1) = 0$, $x = 1/2$. However, no definitive conclusions can be drawn because of the lack of data near the melting point.

Combinations of all of these models, i.e., a partially ionized, partially undissociated liquid state could be formulated but the arbitrariness of such a model makes it of doubtful value even with good data near the melting point. The point to be emphasized is that even in the first approximation of an ideal liquid, considerable choice is available in the models one can consider. It is suggested that of the two simplest models for compounds like CdS, an undissociated liquid state may be the better first approximation.

It is noted that the general thermodynamic relationships on which Eqs. (1) and (2) are based are valid over the composition range from the melting point to the A - AB (Cd-CdS) eutectic. Thus, assuming that the heat of fusion is independent of temperature, these equations give the temperature dependence of x in the limit of small sulfur composition. Viewed this way, Eqs. (1) [or (2)] represent the temperature dependence of the solubility of sulfur in Cd [or of CdS in Cd]. The straight line portion of Fig. 2 verifies the regularity of the liquid for small x . Hence, a straight line extrapolation of the curves in Fig. 2 should be valid to the Cd-CdS eutectic. If these curves are extrapolated to the temperature corresponding to the Cd melting point as an upper

limit of the eutectic temperature, a sulfur composition of the order 10^{-12} is calculated. This indicates that the Cd-CdS eutectic is immeasurably different from the Cd melting point and that the extrapolation itself is valid to any measurable composition value.

The data as presented in Fig. 2 gives a plot similar to that found for the III-V semiconducting compounds. Specifically, within the experimental errors, the value of ΔS determined from the slope of the lines drawn in Fig. 2, $18 \text{ cal deg}^{-1} \text{ mole}^{-1}$, is identical to the value found for III-V semiconducting compounds.⁴ This implies that the change in randomness upon melting is the same for these types of compounds. Since the solids of these compounds are crystallographically similar (tetrahedral arrangements of atoms), this seems to imply that their liquid states are similar also.

ACKNOWLEDGEMENTS

The author thanks R. N. Hall and J. S. Prener for comments. He is particularly grateful to M. R. Lorenz for discussions on the subject of this paper. B. B. Binkowski assisted in the experimental work. M. Aven suggested ways of mechanically separating the Cd from the CdS.

REFERENCES

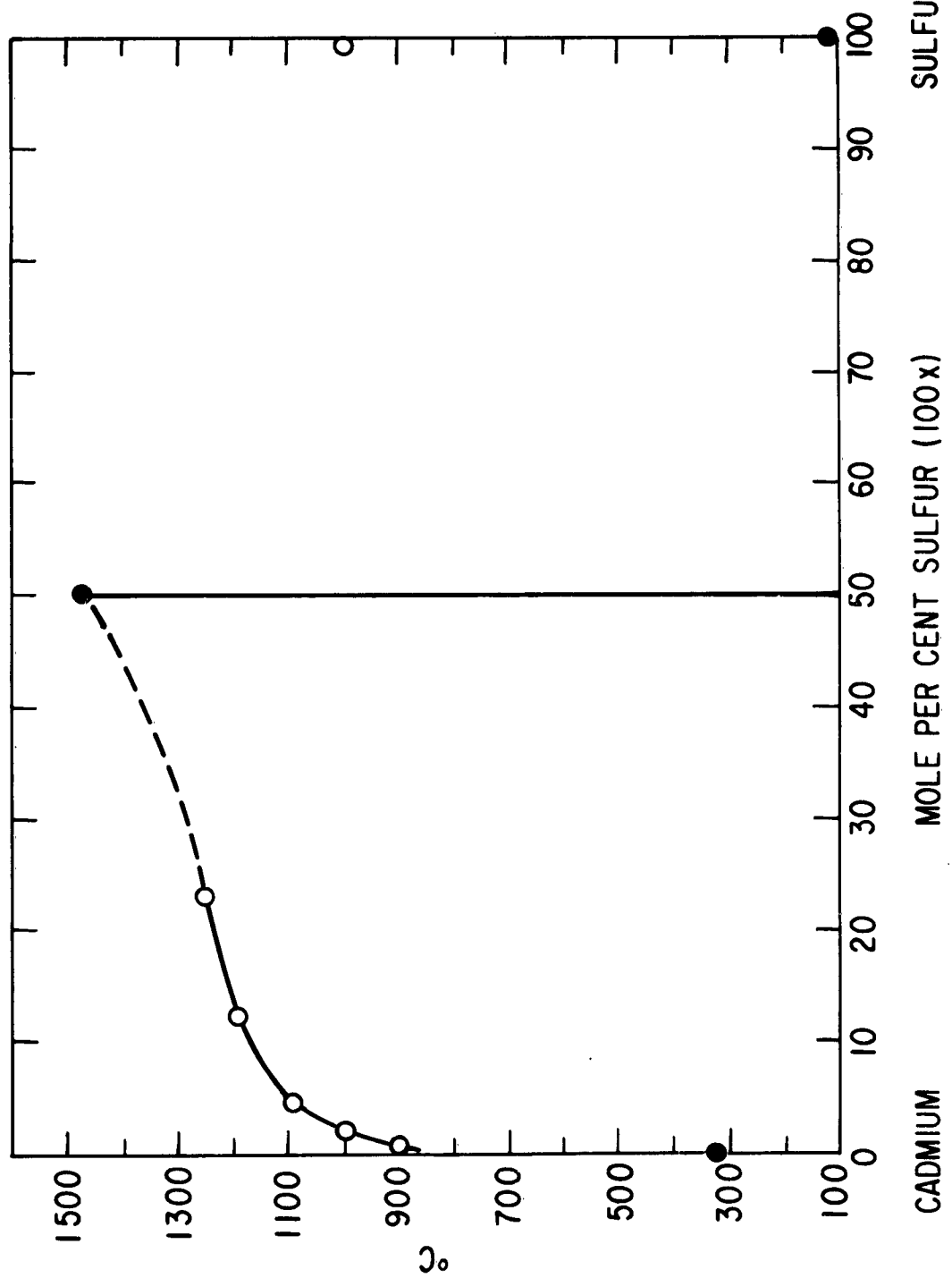
1. M. Aven and H. H. Woodbury, *Appl. Phys. Letters* 1, 53 (1962).
2. A. Addamiano, *J. Phys. Chem.* 61, 1253 (1957).
3. G. Wagner, *Acta Met.* 6, 309 (1958); W. F. Schottky and M. B. Bever, *Acta Met.* 6, 320 (1958); L. J. Vieland (to be published).
4. R. N. Hall, *J. Electrochem. Soc.* (to be published).

FIGURE CAPTIONS

Figure 1 Phase diagram of CdS showing portion of the Cd-CdS liquidus that has been measured. The melting point of CdS is taken from Ref. 2. The one point on the sulfur rich side at 1000°C corresponds to a Cd solubility of $0.1 \pm 0.1\%$.

Figure 2 Dimensionless plot of Cd-CdS liquidus where x is the sulfur composition at temperature T . T_m , the melting point of CdS, and T are in °K. See the text for a discussion of the choice of the ordinate function.

FIG. I



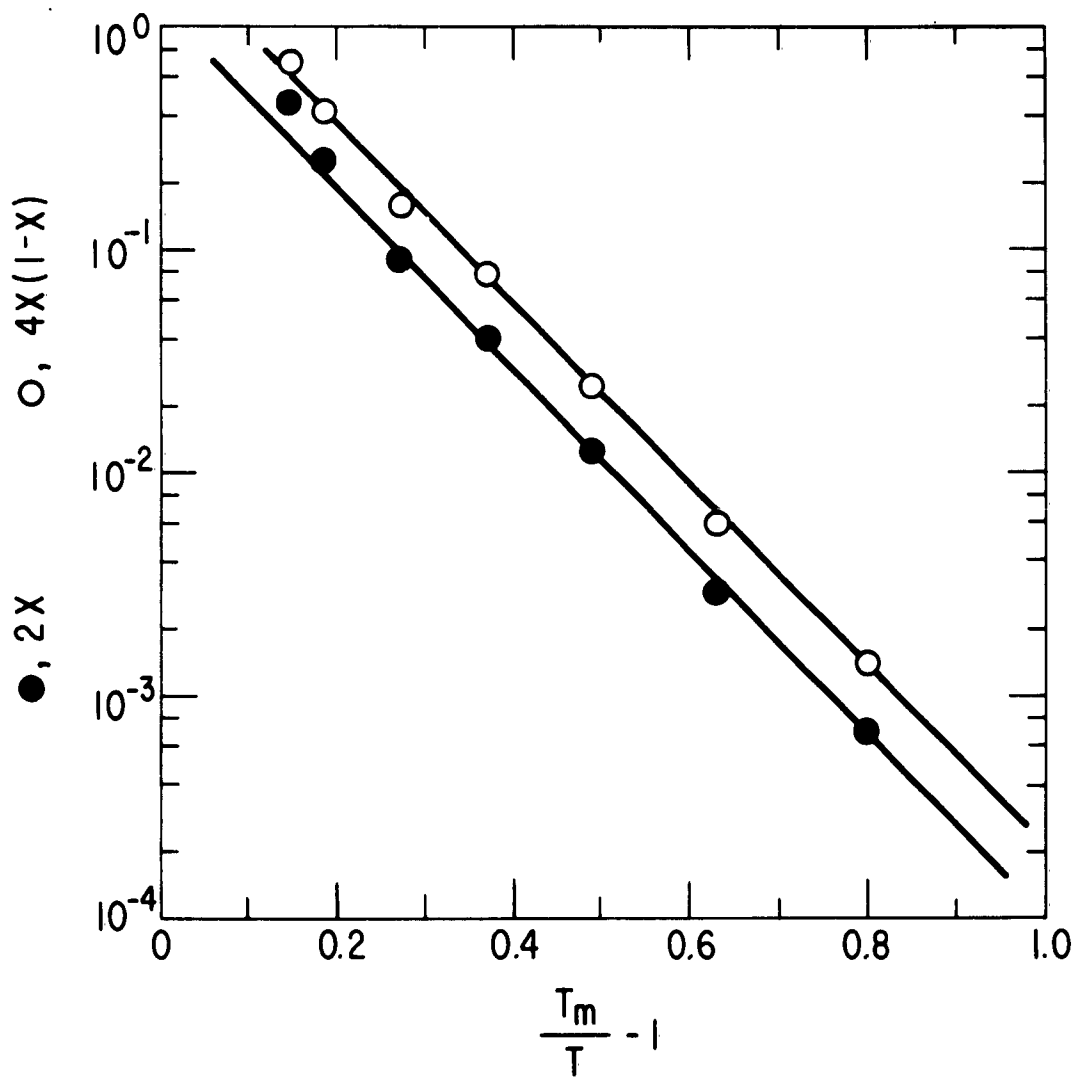


FIG. 2

C. A DOUBLE ACCEPTOR DEFECT IN CdTe* (M. R. Lorenz and H. H. Woodbury)

In the course of studying the electrical properties of high-purity single crystals of CdTe, a new center, thought to be a native double acceptor, has been observed. It is believed to be the first of its kind in compound semiconductors identified by electrical transport measurements. This center is formed during heat treatment in a Cd atmosphere. The doubly ionized acceptor level lies 0.056 ev below the conduction band and when this level is filled the center contains two electrons and is an effective hole trap at low temperatures. In fact, the singly negatively-charged center has such a low cross section for electron capture that it is impossible to observe a normal freeze out of electrons into the second level when the samples are cooled below a critical temperature region. A similar level about 0.09 ev below the conduction band has also been found in CdS.

CdTe samples were prepared by techniques already described.¹ High-purity crystals having a residual impurity donor concentration of about 10^{15} cm⁻³ were used.² Hall bars of approximately 3 x 3 x 10mm³ were sealed in small evacuated quartz ampoules to which Cd metal was added. These were heated to various temperatures for varying lengths of time and then quenched. The surface regions of the samples were removed by grinding, etching, and a final chemical polish. The crystals were then studied using conventional d.c. techniques to measure the Hall coefficient, resistivity, and Hall mobility from 350°K to 12°K. There

* The research reported in this paper was supported in part by the Aeronautical Research Laboratory, Office of Aerospace Research, United States Air Force, and in part by the Air Force Cambridge Research Laboratories, Office of Aerospace Research, under Contract AF19(628)-329

were provisions for exciting the samples with a small incandescent lamp mounted inside the cryostat.

The temperature dependence of the Hall constant for electrons in several samples is shown in Fig. 1. Curve A represents an unfired samples; curve B, a sample fired at 900°C for 30 min.; and curve C, a sample fired at 900°C for 285 hrs. The solid curves correspond to measurements without light and the dotted curves show the effects following photoexcitation at the lowest temperature. Freeze out of electrons into the level of interest starts near 300°K and is most pronounced in curve B. The thermal activation energy is 0.056 ev. At about 110°K the electronic equilibrium starts to lag the thermal equilibrium. The lag increases as the temperature is lowered and at 85°K it is necessary to wait several hours to establish electronic equilibrium. At lower temperatures it becomes impossible to reach equilibrium with regard to the 0.056 ev level. This sluggishness was observed for the heating as well as the cooling of samples in this temperature region.

The peculiarity of the above behavior suggests that a barrier is associated with the 0.056 ev level. The decay of conduction electrons following photoexcitation was measured at four temperatures in the critical temperature region, i.e., 95 to 115°K. The simple relation $\Delta n = c \exp(-t/\tau)$ was observed over three decades at each temperature and over the limited temperature region the lifetime can be expressed as $\tau = \tau_0 \exp(0.27 \text{ ev}/kT)$, where $\tau_0 = 3.2 \times 10^{-12} \text{ sec.}$

In Fig. 2 the Hall mobilities are shown corresponding to the Hall constants of Fig. 1. Curve A again is the unfired sample which also exhibits the intrinsic mobility over the range shown.² Photoexcitation did not change the mobility for this sample. There is, however, a pronounced effect on the mobility of the fired samples, as seen from the dashed curves. After photoexcitation at the lowest temperature, the mobility shows a marked increase. The original mobility curve is rejoined at about 100°K, the temperature at which the excess electrons, thrown out of equilibrium at the lowest temperature, are able to freeze into the 0.056 ev level.

We conclude that the 0.056 ev level, although close to the conduction band, is the doubly ionized state of a two-level acceptor defect. The singly ionized state has a charge of (-1) and is responsible for the barrier observed. Photoexcitation at the lowest temperature produces hole-electron pairs. The holes are captured (trapped) by the filled double acceptor centers resulting in a change of the charge state of the centers from (-2) to (-1). The excess electrons are unable to reach electronic equilibrium with the centers because of insufficient kinetic energy to surmount the barrier about the singly occupied defect. When the temperature is raised to the critical region, the Hall constant increases and the mobility decreases to their original values as electronic equilibrium is re-established.

The explanation of the behavior observed in these crystals is based on a double acceptor model analogous to that established for many impurities in Ge.³ Qualitatively, the observed effects on mobility and Hall coefficient with and without light show a one-to-one correspondence

between the effects reported here and those reported, for example, for Mn-doped Ge.⁴ A quantitative difference appears to be that in the present case, the ratio of the barrier to the second (thermal) ionization energy is much greater than the ratio seen for double acceptors in Ge. This prevents thermal equilibrium from being established as the CdTe samples are cooled but causes no difficulty for the double acceptor centers seen in Ge.

It is to be emphasized that the double acceptor centers described here are not necessarily the dominant defects in the CdTe system. Under the present preparative conditions their formation is accompanied with a concurrent formation of donor centers. The results indicate that for short firing times the samples are slightly more n-type than they were originally but are also more compensated. Hence, the 0.056 ev level appears to be dominant. After long periods of firing the concentration of both acceptor and donor defects increase, but the latter more than the former. There is an additional peculiarity in this system. Short firing times of about one-half hour produce, after surface region removal, a homogeneously-changed sample. Long firing times of several hundred hours also yield homogeneous samples. However, treatment times of intermediate periods result in inhomogeneous crystals. This suggests that at least two processes occur during heat treatment. The fast one is essentially complete after a short time and then is succeeded by a much slower process.

The following evidence strongly suggests that the double acceptor center described here is a native defect. It is observed only when samples were quenched and is seen in excess of the number of donors and acceptors normally found in slow cooled or annealed samples. Spectroscopic analysis

on CdTe has revealed that likely common metal impurities are below the defect concentrations observed. After heat treatment in excess Cd, a similar double acceptor defect with the doubly ionized level 0.09 ev below the conduction band has also been seen in CdS.. Its electrical properties are identical to the center described here in CdTe. Furthermore, CdTe samples showing the behavior illustrated in curve B of Fig. 1 go to high resistance within several days on standing at room temperature. This decay is suggestive of recombination of Frenckel defects or precipitation of Schottky centers. The present results, however, do not permit an unambiguous identification of the native double acceptor center. Although we believe that the center is a simple native defect, we cannot rule out the possibility that the actual defects involved may be complexes of interstitials and/or vacancies or even chemical impurities that are not normally electrically active. However, such complexes must maintain the properties of a double acceptor.

The authors thank their associates for helpful discussions on the observations reported here. They are particularly grateful to Dr. B. Segall and Miss E. L. Kreiger for analysis of the data. B. B. Binkowski and L. H. Esmann assisted in the experimental work.

REFERENCES

1. M. R. Lorenz and R. E. Halsted, J. Electrochem. Soc., April 1963 (to be published).
2. B. Segall, M. R. Lorenz, and R. E. Halsted, Phys. Rev., March 15, 1963 (to be published).
3. See, for example, W. W. Tyler and H. H. Woodbury, Phys. Rev. 102, 647 (1956).
4. Compare Figs. 11 and 10 of Ref. 3 with Figs. 1 and 2, respectively, of this letter.

FIGURE CAPTIONS

Fig. 1 The temperature dependence of the Hall coefficient, R_H , of n-type CdTe samples. The dashed curves show R_H after photo-excitation at the lowest temperature.

A - original high-purity material.

B - Cd fired for one-half hour at 900°C.

C - Cd fired for 285 hours at 900°C.

Fig. 2 The electron Hall mobility, μ_H , of the samples shown in Fig. 1.

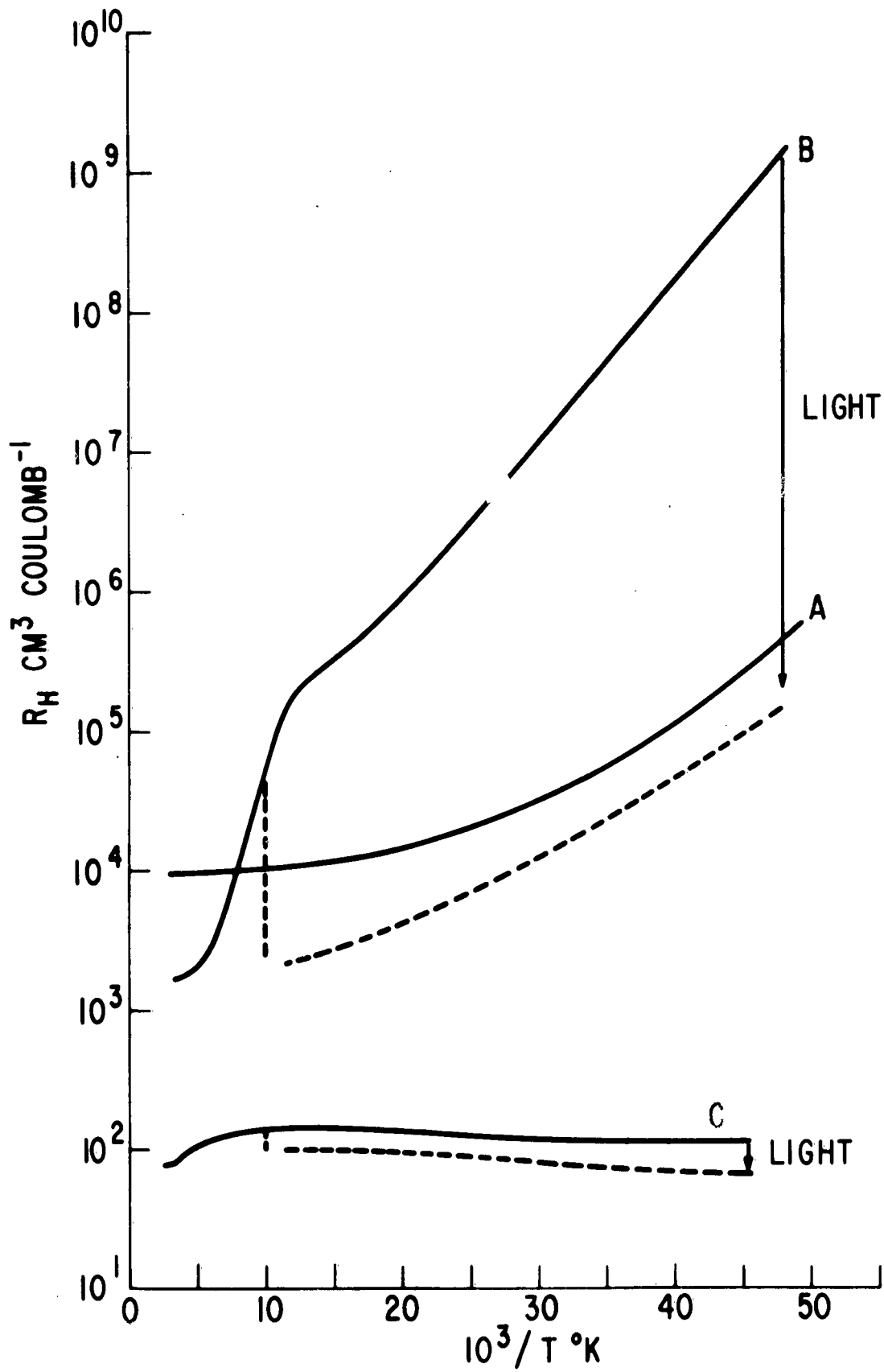


FIG. I

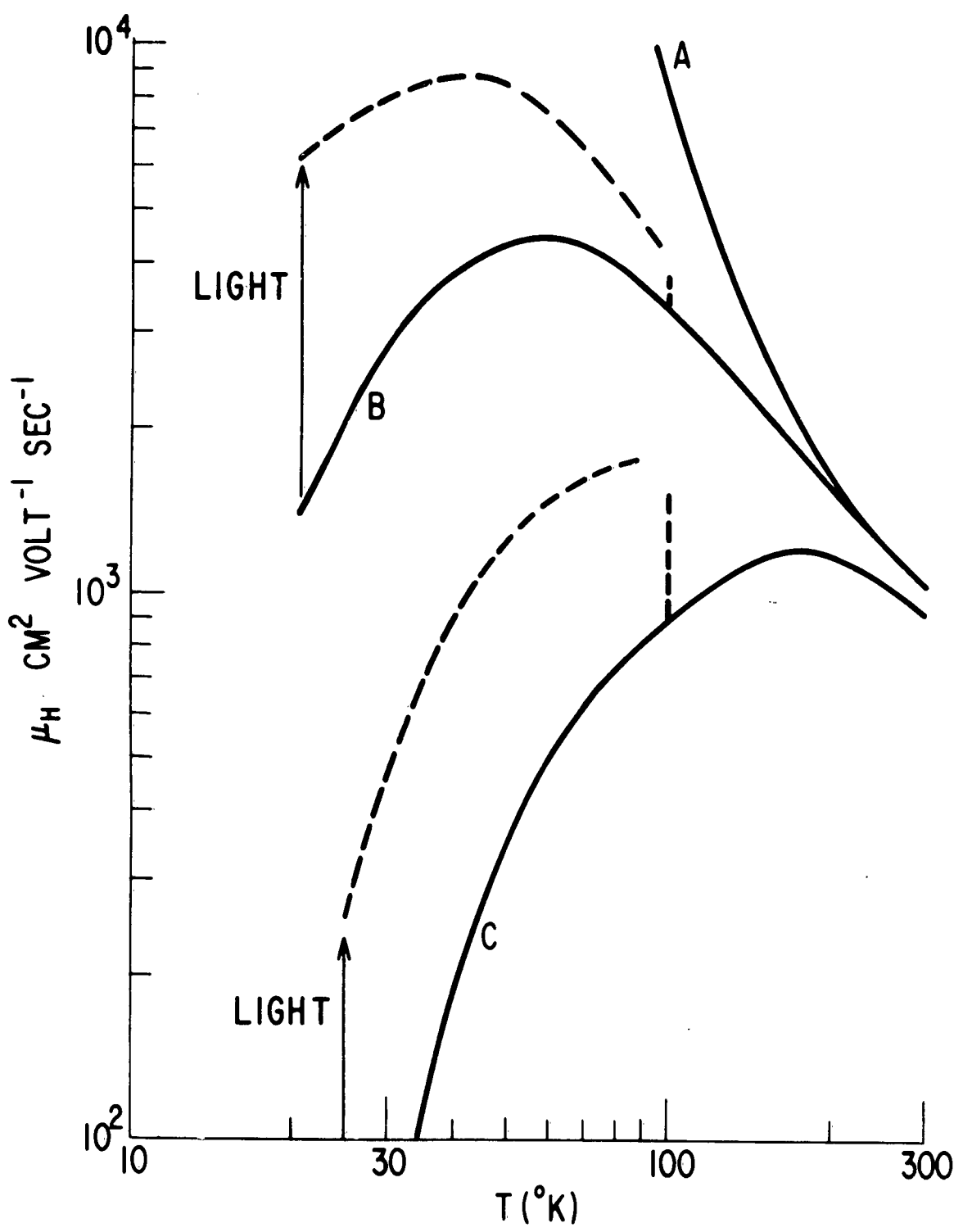


FIG. 2

D. DONOR AND ACCEPTOR CENTERS IN Al-DOPED ZnSe (M. Aven)

INTRODUCTION

In Scientific Report No. 2A under the present contract¹ transport measurements on ZnSe and ZnTe were described and used to analyze the carrier scattering mechanisms and the characteristics of shallow impurity states in these compounds. While it was possible to provide a fairly good identification of the observed acceptor states in ZnTe, the species responsible for the n-type conductivity in ZnSe remained unknown. As the information about the identity of these centers is useful in ascertaining the basic nature of II-VI compounds, and necessary for the development of electro-optical devices from these materials, a study was undertaken to characterize them by diffusion, luminescence and electrical transport measurements.

EXPERIMENTAL TECHNIQUES AND RESULTS

Material Preparation

The ZnSe crystals used in this study were grown as described in previous reports.² The Hall bars cut from the crystals were fired in molten Zn at 950°C for 16 hours to remove the impurities extractable by this method,³ and doped with Al by firing them in liquid Zn-Al alloys.

The approximate diffusion rate and the segregation coefficient for Al were determined for one alloy composition, namely Zn: 10^{-1} Al (an alloy containing 90 atom per cent Zn and 10 atom per cent Al. Fig. 1 shows a half-slice cut out of a rectangular ZnSe crystal slab after partial diffusion of Al from Zn: 10^{-1} Al into the crystal at 1050°C. The photograph was taken under ultraviolet excitation. The diffusion front

is extremely sharp, and can be seen under ordinary illumination as the line of demarcation between a brown frame and a light yellow central area. Under ultraviolet excitation the former is yellow-luminescent, exhibiting a single gaussian emission band peaking at 2.07 eV. The central area, by contrast, is virtually non-luminescent. The low resistivity region advances toward the center of the crystal at the same rate as yellow-luminescent front. The diffusion coefficient for this process was calculated by using the approximate "step-function" formula given by Dunlap,⁴ i.e.

$$D = \frac{x^2}{4t} \ln \frac{C_o'}{C_o}$$

where x is the distance diffused in the time t , C_o' is the surface and C_o the boundary concentration. In the present case x was taken as the distance between the outer edge of the crystal and the line of demarcation between the yellow-luminescent and non-luminescent areas, t was the time elapsed, and C_o' was determined by chemical analysis for Al in the yellow-luminescent region. The quantity C_o which is not easily obtainable experimentally was estimated to lie roughly between 10^{17} and 10^{20} cm^{-3} . The resulting diffusion coefficient is $(2 \pm 1) \times 10^{-9} \text{ cm}^2/\text{sec}$. It is clear that with such low diffusion rates very long times are necessary to ensure uniform diffusion of Al into ZnSe crystals: a cube-shaped crystal 4 mm on edge, for example, would require nearly a month at 1050°C . Higher temperatures, where the diffusion rate would be expected to be faster, were found unsuitable because of rapid disintegration of the ZnSe crystals.

A ZnSe crystal fired in Zn: 10^{-1} Al at 1050°C until complete diffusion had taken place, was found by chemical analysis to contain $1.6 \times 10^{20} \text{ cm}^{-3}$ Al. From this, one calculates (using volume concentrations) the

segregation coefficient

$$k^0 = \frac{\text{conc. of Al in ZnSe}}{\text{conc. of Al in Zn}} \approx 2.5 \times 10^{-2}$$

As it is not known whether the concentration of $1.6 \times 10^{20} \text{ cm}^{-3}$ is below the solubility limit of Al in ZnSe at 1050°C, the above figure for the segregation coefficient should be regarded as its lower limit.

The ZnSe crystals emerge from the firing in the Zn-Al alloys with room temperature resistivities ranging from 10^{-2} to 10 ohm-cm. When such crystals are fired in vacuum or hydrogen at temperatures above approximately 700°C, their resistance increases. A 30-minute firing at 800°C, for example, will increase the resistivity by a factor of 10^4 to 10^6 in crystals a few mm^3 in size. This indicates that the resistivity change proceeds rather rapidly, with a diffusion coefficient (for the species responsible for the change in resistivity) of the order of $10^{-4} \frac{\text{cm}^2}{\text{sec}}$. The original resistivity of such crystals can be completely restored by a firing in Zn vapor at the same temperature. This suggests that the resistivity increase upon hydrogen firing is due to compensation by Zn vacancies, which diffuse into the crystals during the firing in hydrogen, and are annihilated during the firing in Zn vapor.

Steady State Hall Measurements

Figure 2 shows the Hall coefficient versus temperature curves for a number of Al-doped ZnSe crystals. The curves for the samples with intermediate Al concentrations clearly consist of two segments. At high temperatures the slopes of the curves correspond to an ionization energy of roughly 0.1 eV, while their low temperature portions have ionization energies closer to 0.02 eV. It is also apparent that increasing the

Al concentration in ZnSe* increases the free carrier concentration at all temperatures. The sample fired in Zn: 10^{-1} Al is completely degenerate between 40°K and 400°K. The sample fired in Zn: 3×10^{-2} Al shows a hump around 180°K, with a slight drop in carrier concentration at lower temperatures--an indication of freeze-out into an impurity band. The low temperature portions of the next three curves show that a further decrease in the Al concentration brings about a freeze-out of carriers into a shallow donor level. Judging by the low temperature slopes of these three curves, the ionization energy of the donor level appears to be increasing with decreasing impurity concentration, as observed for a number of other semiconductors.^{5,6}

In order to obtain an estimate of the donor ionization energy and the degree of compensation, the data obtained for the sample fired in Zn: 1.2×10^{-3} Al** was fitted to the usual formula for non-degenerate statistics⁷

$$\frac{n(n + N_a)}{(N_d - N_a - n)} = \frac{N_c}{g} \exp(-E_d/kT),$$

*We are assuming here that the Al concentration in ZnSe increases as the Al-content of the Zn-Al alloys is increased. The quantitative relationship between these variables is presently being checked by a series of chemical analyses.

**The Zn: 1.2×10^{-3} Al sample was chosen for analysis because it could be measured over the widest temperature range, thus allowing to obtain the best estimate of the donor ionization energy.

where n is the free electron concentration, N_d is the concentration of donors having the ionization energy E_d , N_a is the concentration of acceptors, g is the degeneracy factor which for the case of a simple donor has the value of 2, and N_c is the conduction band density of states. In calculating N_c the effective mass ratio used was 0.15.⁸ The obtained value for E_d was 0.023 eV, with $N_d = 2.5 \times 10^{16}$ and $N_a = 2.4 \times 10^{16}$. While the estimate of the ionization energy is probably quite accurate, the values for the N_d and N_a could easily be off by as much as a factor of 2 due to the uncertainty in estimating the point of saturation. The ionization energy for the deeper level was calculated from the Hall data for the crystal fired in Zn: 9.2×10^{-4} Al, which sample exhibited the high temperature slope over the longest temperature interval. The obtained value was 0.11 eV.

Photo-Hall Measurements

Recent work with CdTe and CdS has shown⁹ that under certain preparative conditions these compounds exhibit the presence of a double acceptor center which lies fairly close to the conduction band edge. The shape of the Hall curves in Fig. 2 suggests that such centers may also exist in ZnSe.

Photo-Hall data taken on a ZnSe crystal fired in Zn: 1.2×10^{-3} Al and shown in Fig. 3 appear to substantiate this assumption. The solid curve with squares shows the relationship between the Hall coefficient and temperature in the dark. When the sample

is illuminated briefly at, say, 30°K , the Hall coefficient drops by about two orders of magnitude indicating an increase in the free carrier concentration. This increase is, however, not due to photoconductivity in the usual sense, as the increased conductivity persist without perceptible decay even after the illuminating source is removed. In fact, most of the experimental points on the dashed curve were obtained after but a brief illumination at 30°K . Only at a temperature where the curve starts bending upwards does a perceptible decay of the increased conductivity set in.. For this reason the experimental points on the dashed curve at temperatures higher than about 80°K were obtained with the illumination on permanently. The dashed curve joins the dark curve at about 160°K , indicating that at higher temperatures there is no increase in conductivity with illumination.

Figure 3 also shows the Hall data for a ZnSe crystal with comparable Al-doping which was heated for approximately 100 hours at 950°C sealed in a quartz tube with Zn and CdI_2 . The Zn was added to retard the evaporation of the ZnSe crystal and the CdI_2 (approximately 10^{-3} moles CdI_2 per mole ZnSe) served as a source of I. The solid phases of the Zn and the CdI_2 were kept from making direct contact with the ZnSe crystal. The Hall data for this crystal in the low temperature region are strikingly similar to the illuminated curve of the Al-doped sample: the slopes of

the curves for both correspond to ionization energy of 0.020 eV, the donor concentration in both crystals is about $2 \times 10^{16} \text{ cm}^{-3}$, and the acceptor concentrations lie between 4 and $6 \times 10^{15} \text{ cm}^{-3}$. The compensation ratio in both is about 3 to 4 donors per acceptor. The dark curve for the Al-doped sample, on the other hand, while having a comparable donor concentration, has a compensation ratio of about 1.0^4 donors per acceptor. As expected, the sample doped with Al and I showed very little photoconductivity at all temperatures.

The decay of the excess carrier concentration following photoexcitation was measured in the critical temperature region, i.e., between approximately 90 and 115°K . Because of a rather fast initial drop, followed by a very slow further decrease in carrier concentration, it was not possible to fit the decay curves to a simple kinetic equation over the entire range of decay. It was found, however, that the slow portion of the decay curves could be fitted to a bimolecular reaction formula, i.e..

$$\frac{1}{n} = kt + \frac{1}{n_0} ,$$

where n_0 is the concentration of the excess carriers at time $t = 0$, n is the excess carrier concentration at time t , and k is the decay rate constant. Figure 4 shows the decay curves plotted as the reciprocal of the excess carrier concentration versus time. It can be seen that after the initial fast decay portion the curves

can be satisfactorily fitted to the above equation. Although the temperature range in which these measurements could be carried out is rather limited, it was possible to calculate a rough activation energy by fitting the decay rate constant obtained from Fig. 4 to an Arhennius type equation, i.e., $k = k_0 e^{-\frac{E}{kT}}$. The E obtained from the present data was found to be approximately 0.25 eV. It is noted that this value is very close to the activation energy found in CdTe.⁹ The meaning of this energy is not clear at present.

Figure 5 shows the mobility versus temperature relationship for ZnSe:Al with and without prior illumination, and for ZnSe:Al,I in the dark. It can be seen that the illumination produces a large increase in mobility. As in the case of the Hall curves, the mobility of ZnSe:Al,I is again comparable to that of the illuminated ZnSe:Al suggesting that, in both cases, scattering centers have been modified or removed.

DISCUSSION

It is our objective to use the presented experimental data to derive an energy level scheme for Al-doped ZnSe, and to attempt to assign these levels to definite native or foreign impurities. It will be seen that, while in some cases the identification appears to be quite plausible, there remains much work to be done before the over-all picture can be regarded as satisfactorily understood.

Shallow Donors

The data in Fig. 2 indicate that the free carrier concentration in ZnSe:Al increases with increasing Al concentration. This suggests

that the observed shallow donor is associated with the presence of Al in ZnSe. The simplest model for such a center is a substitutional unassociated Al. If present in sufficiently low concentrations, the ionization energy of such donor species may be estimated from the simple hydrogenic model, i.e.

$$E_d = \frac{e^4}{2 h^2 \epsilon_s^2 m^*},$$

where e is the electronic charge, h is the Planck's constant ($h = \frac{\hbar}{2}$), ϵ_s is the static dielectric constant and m^* is the effective mass of the electrons. Using 8.1^8 for the dielectric constant and $0.15 m_0$ for the effective mass of electrons one obtains 0.031 eV for the hydrogenic donor ionization energy.^{*} The observed donor ionization energy of 0.023 eV is sufficiently close to this value to suggest that the donor level introduced by Al is hydrogenic in nature. The fact that the observed ionization energy is below the calculated value may reflect the dependence of

^{*}The use of the static dielectric constant in the above equation is not strictly valid because of the closeness of the energy of the longitudinal optical phonon (0.031 eV) to the calculated ionization energy. The obtained value should therefore be regarded as only approximately correct.

the ionization energy on the impurity concentration, as has been shown to be the case for, e.g., Ge⁶ even at relatively low impurity concentrations.

Double Acceptor States

The photo-Hall data of Fig. 3 suggests that the sample contains centers close to the conduction band edge which act as hole traps. As the sample is cooled down from room temperature, the carriers first freeze out on this level. At about 160°K the Hall curve bends over indicating freeze-out on the shallow donor level discussed in the preceding section. When the sample is illuminated at low temperatures with light capable of producing electron-hole pairs, a persistent enhanced electron conductivity is observed indicating that there exists a barrier preventing the recombination of the created photoelectrons. The simplest way to explain these data is to assume that the 0.11 eV level is the second acceptor level of a double acceptor defect, as has been postulated for CdS and CdTe.⁹ The donor-acceptor balance of the sample is such that at room temperature this defect contains one electron and is, therefore, singly negatively charged. Between room temperature and approximately 80°K, electrons freeze-out into the second acceptor level. When the sample is subjected to photoexcitation below this temperature, the created holes are

quickly captured by the filled acceptor centers, leaving them in a singly negatively charged state. The electrons, on the other hand, cannot easily recombine with the trapped holes because of insufficient thermal energy to overcome the Coulombic repulsion between them and the singly negatively charged acceptors.

It is of interest to compare the dark and illuminated Hall curves of ZnSe:Al to that of ZnSe:Al, I (Fig. 3). The close correspondence between the Hall curves, the ionization energies and compensation suggest that the treatment to which the ZnSe:Al, I crystal was subjected produced essentially the same effect in this crystal as illumination did in the ZnSe:Al sample--namely the elimination of the double acceptor levels. In the ZnSe:Al, I sample the double acceptors were removed permanently by chemical treatment; in the ZnSe:Al crystals they were converted to singly negatively charged species by photoexcitation.

The removal or modification of the double acceptor states is also reflected in the higher mobilities of ZnSe:Al, I and in the illuminated ZnSe:Al crystal, as illustrated in Fig. 5. The increase in mobility for the illuminated ZnSe:Al sample is, however, larger than one would expect to find merely on the basis of the conversion of doubly charged scattering centers to singly charged ones. One way to explain this is to assume that, superimposed on the above effect, we have a further increase in mobility due to

partial elimination of impurity band conduction (in which the mobility is lower) in the illuminated sample.

There is little concrete evidence as to the identity of the double acceptor center. It has been suggested that it could be the cation vacancy.¹⁰ It has also been proposed (see this report, section on CdS) that, if the compound exhibited a sufficient degree of covalent bonding, an anion vacancy could act as an acceptor. In the present samples both of these species are likely to be present. The experiments demonstrating the loss of conductivity of Al-doped ZnSe crystals after vacuum firing and the restoration thereof following Zn vapor firing, is very suggestive of in- and out-diffusion of Zn vacancies. The fact that, as a rule, even the low resistivity ZnSe samples are highly compensated, indicates, therefore, that Zn vacancies may be the major compensating species in ZnSe. It is somewhat harder to visualize Se vacancies as the compensating species, as firing in Zn vapor would then not be expected to reduce compensation. However, it is possible that the Se vacancies are introduced during the relatively long term firing in Zn-Al alloys, and are diffusing too slowly to play a role in the relatively short term vacuum and Zn vapor firings.¹¹ The fact that the ZnSe:Al sample into which I was diffused had lost most of its double acceptors is not inconsistent with the hypothesis that the double acceptor is a Se vacancy--the I atoms which diffused into

ZnSe could well have filled up a part of the Se vacancies and hence annihilated part of the double acceptor species.

It is also conceivable that a foreign impurity, e.g., Si, may act as the double acceptor. Spectroscopic analyses have shown that the foreign acceptor impurity concentration in the ZnSe crystals is too low for them to act as the major compensating species. The concentration of the double acceptors, however, does not have to be nearly as large as that of the major compensating species for the reported photo-effects to be observed.

Luminescence Centers

There are good reasons to believe that a considerable portion of the incorporated Al is tied up in luminescence centers of the type characterized by Prener and Weil¹² in ZnS. Prener and Weil proposed that the so-called self-activated blue luminescence in ZnSe was due to doubly charged Zn vacancies in nearest neighbor association with halogens or next nearest neighbor association with trivalent donor atoms. Study of the luminescence spectra of solid solutions of ZnS and ZnSe indicate that the self-activated blue band in ZnS shifts towards lower photon energies with increasing Se content, and eventually becomes the yellow emission peaking at 2.07 eV in pure ZnSe.¹³ The fact that the present samples exhibit an emission band peaking at 2.07 eV therefore suggests that the room temperature luminescence of Al-doped ZnSe is dominated by

luminescence centers of the type characterized by Prener and Weil in ZnS. It should be emphasized, however, that no proof can be adduced from the present work as to the state of association of Al with the Zn vacancies.

CONCLUSION

It has been shown that ZnSe can be made to exhibit shallow hydrogen-like donor states 0.023 eV below the conduction band edge by diffusion of Al into the crystals. Along with the incorporation of the donor centers, the in-diffusion of Al is accompanied by the crystals acquiring a yellow fluorescence band peaking at 2.07 eV. The luminescence centers responsible for this emission are similar to the self-activated blue centers in ZnS, which are believed to be due to Zn vacancies, possibly associated with substitutional Al.

The ZnSe: Al samples also exhibit the presence of double acceptor defects in which the second acceptor level is 0.11 eV below the conduction band edge. These centers act as hole traps at low temperatures, allowing photoexcited electrons to stay unrecombined in the conduction band for very long times. The concentration of the double acceptor centers can be significantly reduced in the ZnSe:Al crystals by heating them in Zn and CdI₂ vapor at 950°C. The identity of these centers is not known at the present, the suggested possibilities being Zn or Se vacancies, or Si impurity.

The ZnSe crystals prepared under the specified conditions undoubtedly contain other centers besides the enumerated ones-- fluorescent spectra measured at low temperatures by Halsted,¹⁴ for example, have exhibited several more emission bands than can be accounted for by the above centers. It is believed however, that the major electrical and luminescent properties of Al-doped ZnSe crystals are adequately characterizable by the described species.

ACKNOWLEDGEMENT

The author wishes to acknowledge the contribution of W. Garwacki in materials preparation and the assistance of Miss Elise Kreiger in making the computations. Particular thanks are due to the author's colleagues, R. E. Halsted, M. Lorenz, B. Segall and H. H. Woodbury for the many stimulating discussions in the course of this study.

REFERENCES

1. Air Force Cambridge Research Laboratories Contract No. AF19(628)-329, Scientific Report No. 2A.
2. Air Force Cambridge Research Laboratories Contract No. AF19(604)-8512, Report No. 1 (1961).
3. M. Aven and H. H. Woodbury, Appl. Phys. Letters 1, 53 (1962).
4. W. C. Dunlap, Jr., Phys. Rev. 94, 1530 (1955).
5. W. W. Piper and R. E. Halsted, Proc. Intern. Conf. on Semicond. Phys., Prague (1960), p. 1046.
6. P. P. Debye and E. M. Conwell, Phys. Rev., 93, 693 (1964).
7. See, for example, T. H. Geballe, Semiconductors, ed. by N. B. Hannay, Reinhold Publ. Corp., New York (1959), p. 313.
8. M. Aven, D. T. F. Marple and B. Segall, J. Appl. Phys., 32, 2261 (1961). For a more recent effective mass determination: D. T. F. Marple (personal communication).
9. M. Lorenz and H. H. Woodbury, Phys. Rev. Letters (to appear in the March 15, 1963 issue).
10. M. Lorenz, personal communication; see also W. Hoogenstraaten, Philips Research Rep. 13, 1952 (1958).
11. A similar argument was used by H. H. Woodbury to explain some of his experimental findings in CdS.
12. J. S. Prener and D. J. Weil, J. Electrochem. Soc. 106, 409 (1959).
13. R. E. Halsted, U.S. Army Eng. Res. and Dev. Laboratories Contract No. DA-44-009 ENG-5172 (1962).
14. R. E. Halsted, personal communication.

FIGURE CAPTIONS

- Fig. 1** Half-slice cut out of a rectangular ZnSe crystal slab under ultraviolet excitation after partial diffusion of Al into the crystal at 1050°C. The width of the yellow-luminescent frame is approximately 1 mm.
- Fig. 2** Temperature dependence of the Hall coefficient for ZnSe crystals fired in Zn-Al alloys of different Al concentrations.
- Fig. 3** Temperature dependence of the Hall coefficient for a ZnSe:Al crystal in the dark and following photoexcitation, and for a ZnSe:Al, I crystal in the dark.
- Fig. 4** Decay of excess carriers in ZnSe:Al crystals following photoexcitation at the indicated temperatures. The decay constants, k, were calculated from the slopes of the straight line portions of each curve, and conform to the formula $\frac{1}{n} = kt + \frac{1}{n_0}$.
- Fig. 5** Temperature dependence of the mobility for a ZnSe:Al crystal in the dark and following photoexcitation, and for a ZnSe:Al, I crystal in the dark.

YELLOW-LUMINESCENT
RESISTIVITY $\sim 10^{-2} \Omega\text{-cm}$.

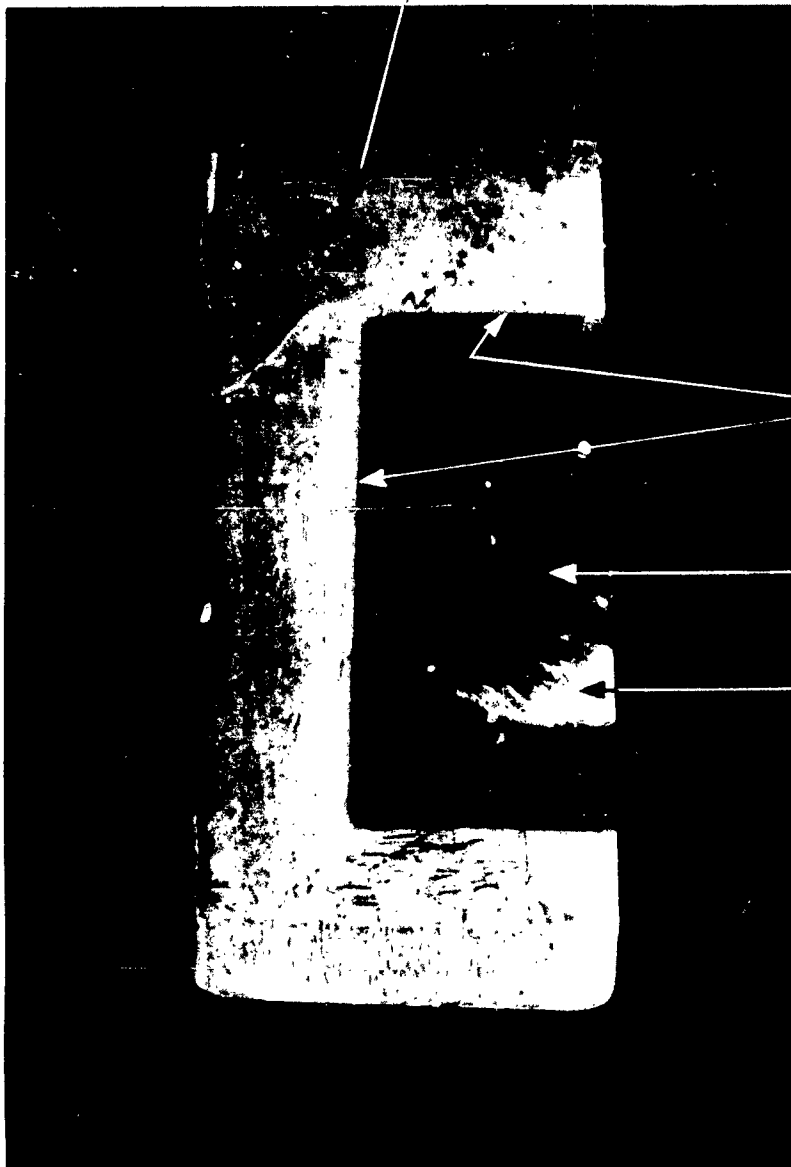


FIG. 1

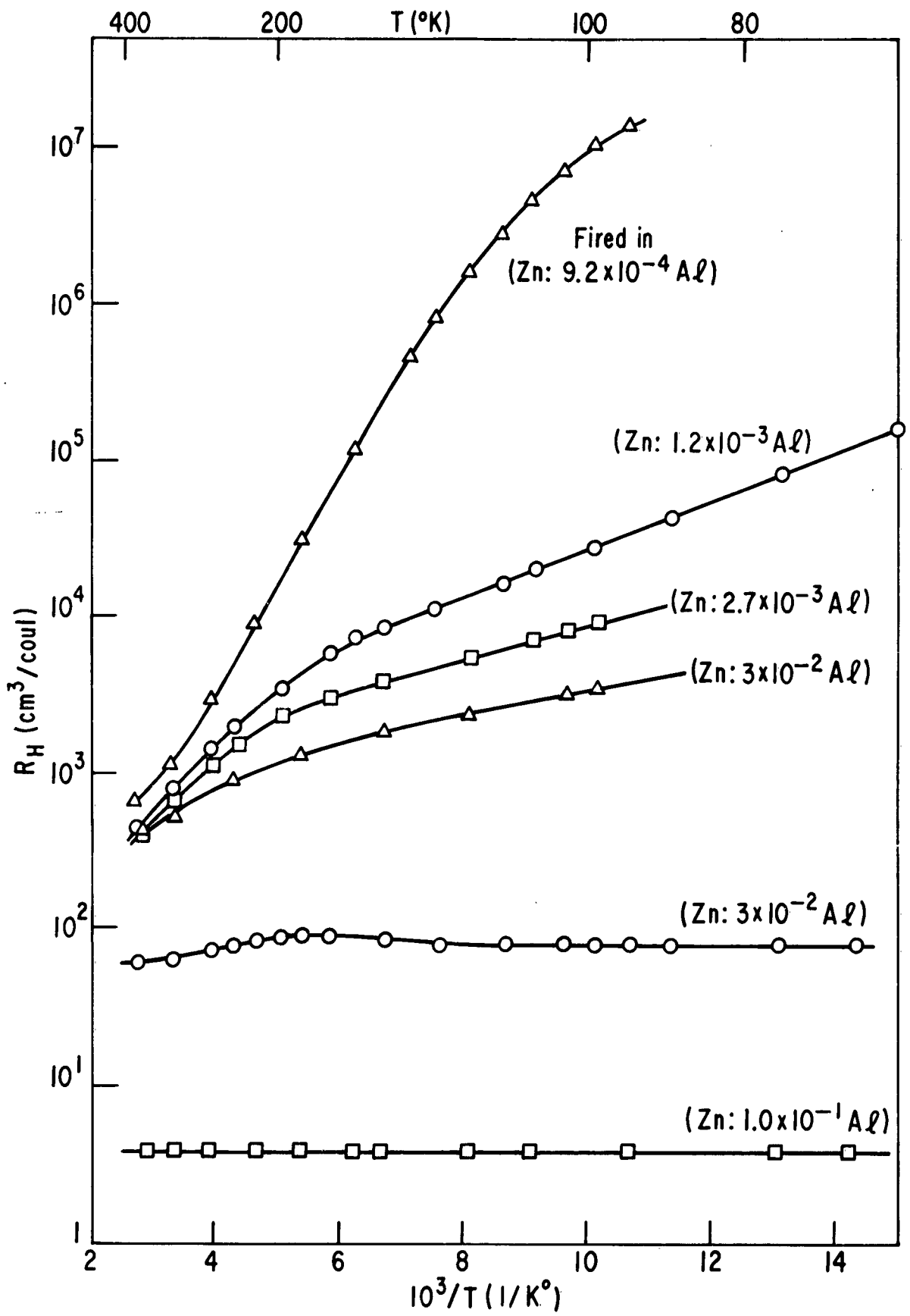


FIG. 2

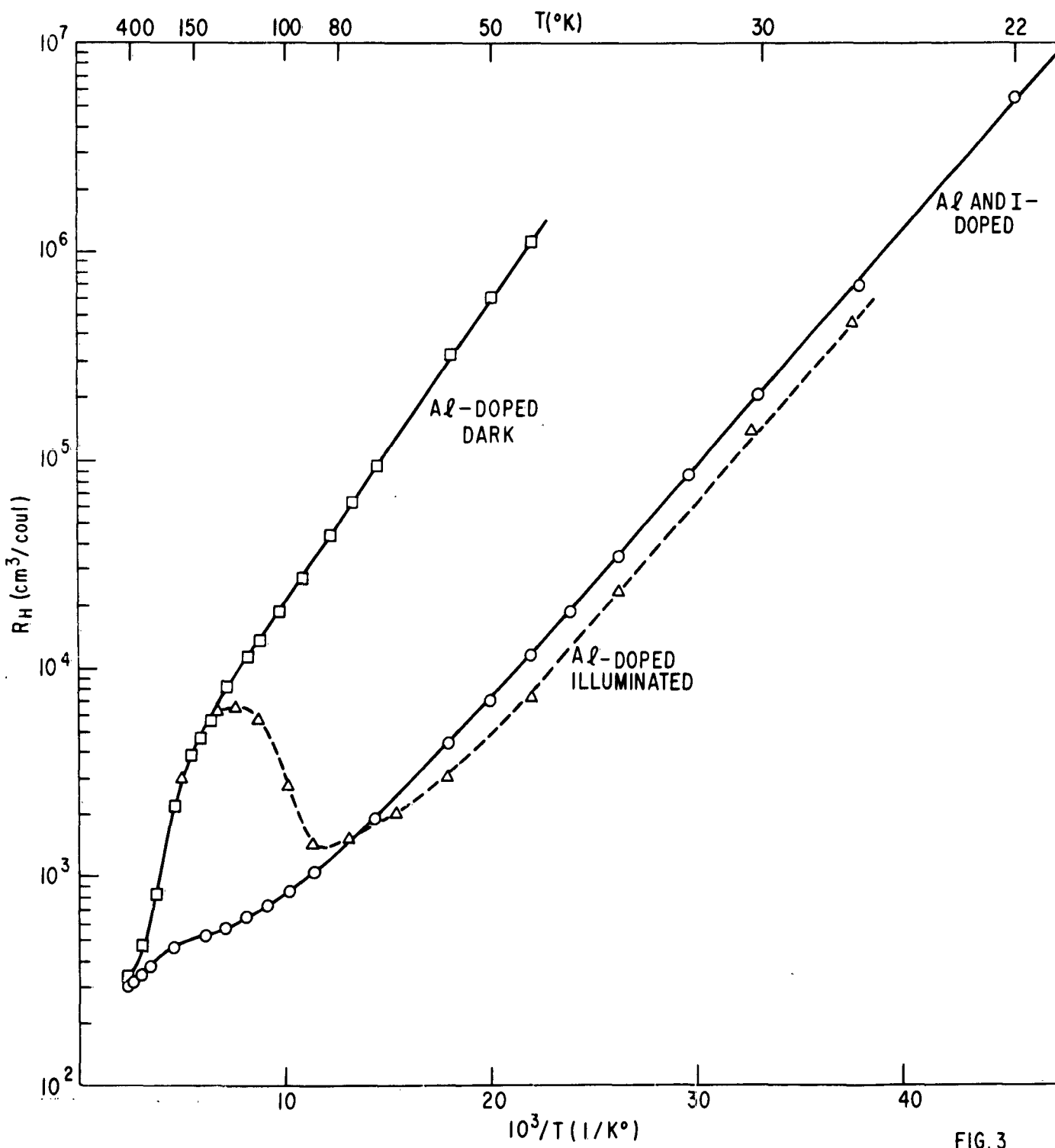


FIG. 3

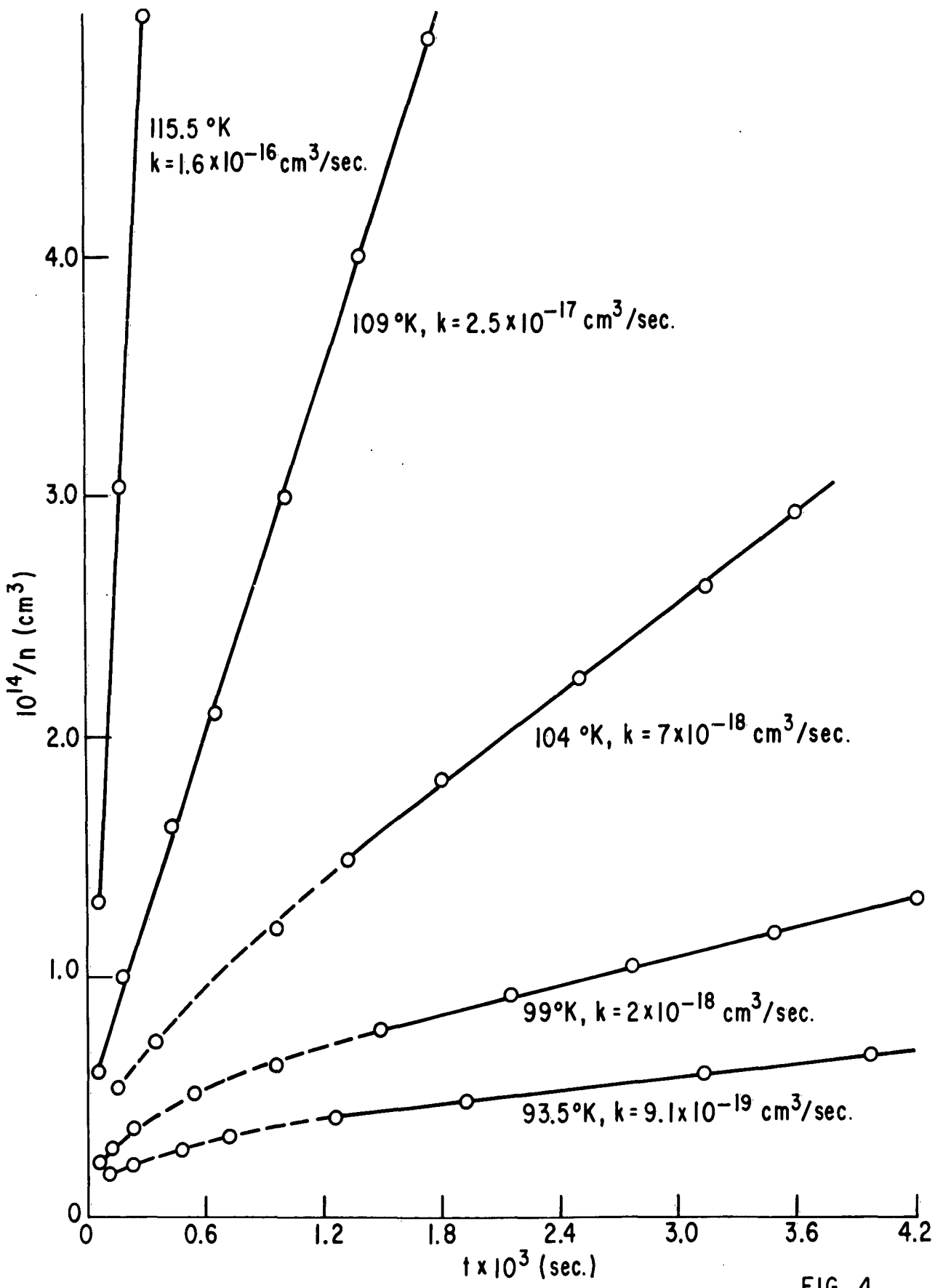
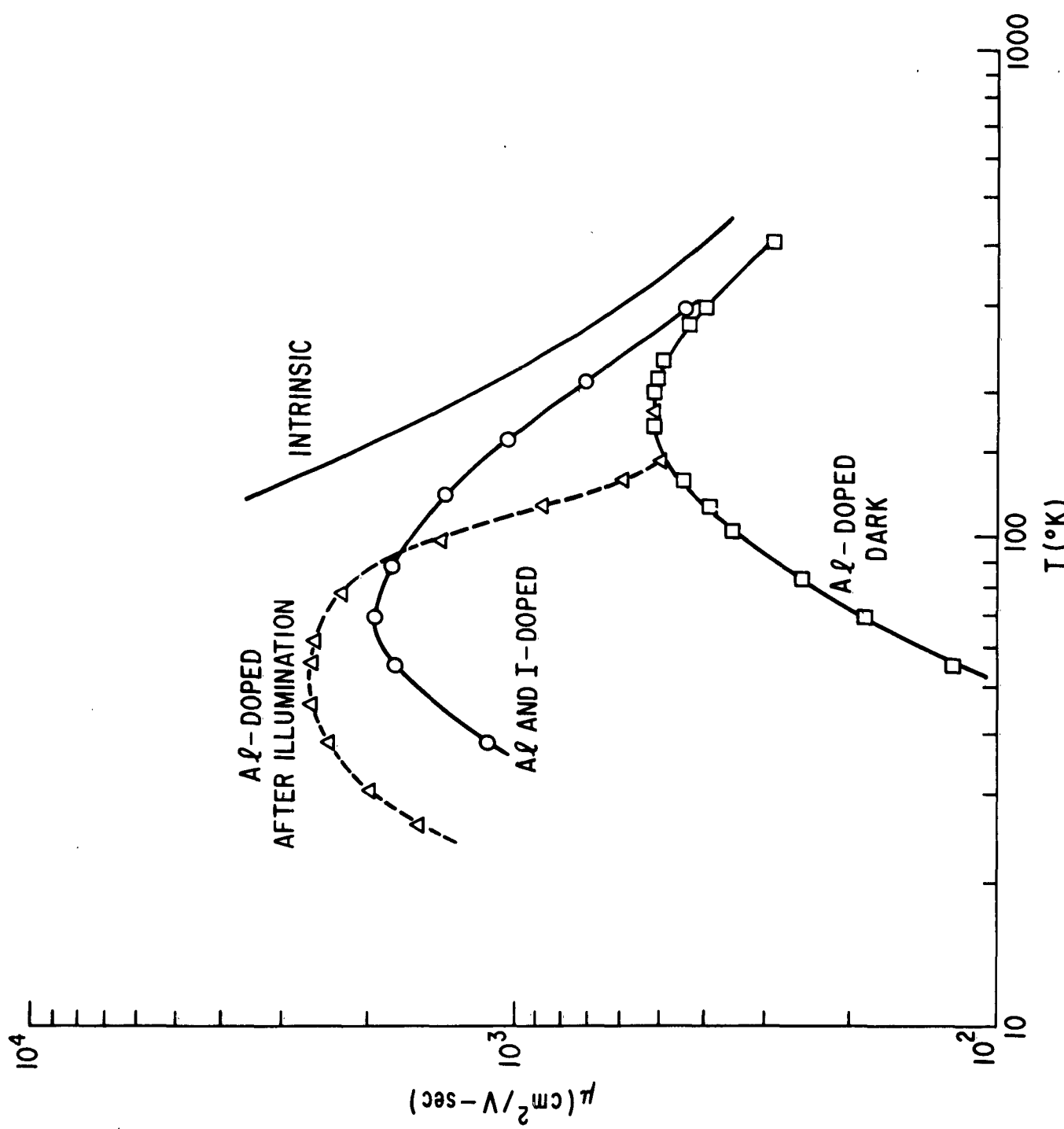


FIG. 4

FIG. 5



E. RADIATION FROM GaSb AND GaAs_xP_{1-x} JUNCTIONS (J. H. Racette)

Further investigation of the recombination radiation from diffused gallium antimonide junctions has shown that at least two peaks are present, one centered around 1.6μ , the other about 1.7μ at 77°K and lower. The amplitude of the latter peak has been found to vary linearly with the current through the junction. The relative amplitudes of these peaks varies from diode to diode. In some diodes the amplitude of the 1.6μ radiation peak increases with a greater than linear dependence upon diode current (supralinearity). The width of this peak at half-maximum amplitude is 0.07μ , while the longer wavelength peak is 0.16μ wide. The wavelength shift at low currents noted in the previous report is associated with the 1.7μ peak. More thorough study of GaSb junctions is in progress.

Planar Zn-diffused junctions having junction widths in the range 600 to 1200\AA have been prepared from halogen transported gallium arsenide phosphide obtained from another group in the Research Laboratory. This material has a composition of 65% GaAs, and a donor concentration of 10^{18} tellurium atoms/cm³.

Although diodes fabricated from these junctions produced bright visible radiation and had excellent current voltage characteristics, no laser action was observed when they were pulsed to 2.5×10^4 amperes/cm² at 77°K and 4.2°K . The light output was linearly dependent upon the diode current. Observation of the GaAs_xP_{1-x} material currently grown in this laboratory

using transmitted infrared light has shown substantial improvement over the quality of earlier samples. However they still show evidence of considerable strain and, in general, a large number of inclusions.

F. ANALYSIS OF THE BAND-TO-BAND MODEL FOR THE JUNCTION LASER
(R. N. Hall)

At present there is considerable uncertainty about the nature of the transition which produces the luminescence in GaAs junction lasers. Calculations have been made of the threshold current, based upon the assumption that the initial and final electron states are essentially discrete in energy.¹ We feel that such a model may not be appropriate, particularly for the more heavily doped laser junctions where the substrate donor concentration may be as high as $6 \times 10^{18} \text{ cm}^{-3}$. Accordingly, we have undertaken an analysis of the threshold conditions for a laser in which the radiation is assumed to be produced by free electron and hole recombination. The results are expressed in terms of experimentally measurable parameters. To the extent that these parameters are presently known, the agreement with observed laser characteristics is considered to be satisfactory. A preliminary outline of this analysis is presented below.

Definitions

$\epsilon = h\nu - E_g$ = energy in excess of band edge, see Fig. 1

ζ = Fermi Energy, see Fig. 1

$x = \epsilon/kT$

$y = \zeta/kT$

α = average absorption coefficient in n and p-type regions

$\alpha_0 = b\epsilon^{1/2}$, absorbtion coefficient for direct band-to-band transitions.

b = defined by α_0

C = density of states per unit ϵ .

e = electron charge

J = Threshold current density

μ = average mobility of electrons and holes in degenerate GaAs.

λ = wavelength of light of energy E_g in GaAs.

θ = 0.86 ratio of heavy hole mass to sum of electron and heavy hole masses.

f_c = $1/[1 + \exp \theta(x-y)]$, Fermi factor for electrons.

f_v = $1/[1 + \exp (1-\theta)(x-y)]$, Fermi factor for heavy holes.

$x_1(y)$ = value of x for which $x^{1/2} f_c f_v$ reaches a maximum.

(spontaneous emission maximum)

$x_2(y)$ = value of x for which $x^{1/2}(f_c + f_v - 1)$ reaches a maximum.

(energy of coherent light emission)

$z(y)$ = maximum value with respect to x of the function,

$x^{1/2}(f_c + f_v - 1)$.

Assumptions

1. The light emission results from direct (vertical in k-space) transitions between conduction and heavy hole valence bands, and these bands are parabolic in accord with the masses in pure GaAs. The light hole valence band is ignored. Screening is sufficient to obliterate any exciton effects. Impurity bands and band-edge tailing are considered to have negligible effect.

2. Electrons and holes are injected in equal concentrations into the active layer of the junction, which has an effective thickness, w , which will be calculated. The current density is calculated using the diffusion equation, modified to take into account degenerate statistics.

3. Band-to-band radiative recombination is assumed to be the dominant recombination process; i.e., the quantum efficiency is taken to be unity.

4. Reflection losses at the resonator faces are neglected.

5. The absorption coefficient α in the passive regions bounding the junction is constant over the spectral region of interest. Actually, α may change appreciably over the energy range of 10 or 20 mev in the vicinity of the band edge which is involved, and a modification of the analysis may be required to take account of this.

6. The threshold current is taken to be equal to the spontaneous recombination current at the threshold injection level. Thus the current through the junction is assumed to be increased by a negligible amount by the onset of stimulated emission. This current density corresponds to the average current density as commonly observed in present junctions, rather than the much higher current densities which may perhaps occur on a microscopic scale in the vicinity of the "hot spots" which are seen under lasing junctions.

Assumptions 3 and 4 may be eliminated by minor extensions of this analysis.

Analysis

The threshold conditions given by McWhorter² and by Hall and Olechna³ for TM and TE waves are used. The conversion from the notation of ref. (2) to that used here is,

$$a \rightarrow w/2$$

$$\sigma_1/\omega \rightarrow \lambda \alpha_o (f_c + f_v - 1)/2\pi$$

$$\sigma_2/\omega \rightarrow \lambda \alpha/2\pi$$

Below we find that $\pi w/\lambda \gg 1$, in which case both polarization directions have the same threshold condition which takes the form,

$$x^{1/2} (f_c + f_v - 1) = \frac{1}{b\sqrt{kT}} \left(\frac{3\lambda^2 \alpha}{\pi^2 w^4} \right)^{1/3} \quad (1)$$

This is to be fulfilled at that part of the spectrum which reaches threshold first, which will occur at the maximum value of the quantity on the left, $z(y)$, a function that may be readily evaluated.

$$z(y) = \frac{1}{b\sqrt{kT}} \left(\frac{3\lambda^2 \alpha}{\pi^2 w^4} \right)^{1/3} \quad (2)$$

Two additional equations may be produced to relate $y=\xi/kT$, w , and the threshold current density, J .

By assumption 6, this current density is equal to the spontaneous recombination rate integrated over the active region,

$$\begin{aligned}
 J &= \frac{8\pi e w}{h\lambda^2} \int_0^\infty b\epsilon^{1/2} f_c f_v d\epsilon \\
 &= \frac{8\pi e b w (kT)^{3/2}}{h\lambda^2} \int_0^\infty x^{1/2} f_c f_v dx
 \end{aligned} \tag{3}$$

This last integral is a function of y alone, and may also be evaluated.

We also have the diffusion equation (assumption 2) for the current.

$$J = enD/w$$

$$= 4eC \zeta^{5/2} M/9w \tag{4}$$

using appropriate expressions for the electron concentration, n , and the diffusion coefficient, D , in degenerate material.

To solve these three simultaneous equations, we first eliminate J between (3) and (4) and then substitute the expression for w^2 so obtained into (2). We find,

$$w^2 = \frac{h\lambda^2 \mu C k T}{18\pi b} y^{5/2} \left[\int_0^\infty x^{1/2} f_c f_v dx \right]^{-1} \tag{5}$$

and

$$\frac{12\sqrt{3} \alpha^{1/2}}{b^{1/2} C u h \lambda (kT)^{7/4}} = \frac{2 z^{3/2} y^{5/2}}{3 \int_0^\infty x^{1/2} f_c f_v dx} \tag{6}$$

The left side of this equation consists of known quantities and can be evaluated directly. The right side involves only the variable, y , which can thus be evaluated, and hence the Fermi energy, ζ , corresponding to the threshold conditions is determined. We then obtain w from (5), and J from either (3) or (4).

Curves of J , w , and ζ against T are shown in Fig. 2, for the following choices of the variables.

$$\alpha = 100 \text{ cm}^{-1} \text{ and } 400 \text{ cm}^{-1}$$

$$b = 2 \times 10^4 \text{ cm}^{-1} \text{ ev}^{-1/2}$$

$$c = 1.46 \times 10^{20} \text{ ev}^{-3/2} \text{ cm}^{-3}$$

$$\mu = 400 \text{ cm}^2 \text{ ev}^{-1} \text{ sec}^{-1}$$

$$\lambda = 2.4 \times 10^{-5} \text{ cm.}$$

These calculated current densities are the same order of magnitude as are observed experimentally. The temperature dependence is more gradual, J being approximately linear with T at high temperatures, whereas a T^3 dependence is more typical of actual lasers. Presumably this is due to taking constant values for the above parameters, whereas some of them may vary considerably with temperature. For example, the high α in p-type GaAs may be due primarily to indirect (phonon-assisted) transitions from the Fermi surface to the bottom of the conduction band, in which case the absorption would increase rapidly with temperature as the population of the appropriate phonons increases.

At low temperatures, $y \rightarrow \infty$, and the right side of Eq. (6) approaches $y^{7/4}$. In the limit, we obtain,

$$\zeta_0 = \left[12\sqrt{3} \frac{\alpha^{1/2}}{C_m h \lambda b^{1/2}} \right]^{4/7} \quad (7)$$

$$w_0^2 = \frac{h \lambda^2 \mu C}{12 \pi b} \zeta_0 \quad (8)$$

$$J_0 = \frac{8}{3} \sqrt{\frac{\pi}{3}} \frac{e}{\lambda} \left(\frac{b C M}{h} \right)^{1/2} \zeta_0^2 \quad (9)$$

Thus, a finite threshold current is obtained at $T=0$, as indicated by experimental data.

It is to be noted that Eq. (5) predicts that w will increase gradually with increasing Fermi energy as the threshold current is approached. Undoubtedly, w will decrease again near threshold as stimulated emission becomes important, but this effect is not included in the analysis in its present form. The magnitude of $w (\approx 1\mu)$ is such as to make the quantity $\pi w / \lambda$ large compared with unity, justifying the condition mentioned at the beginning of the Analysis section.

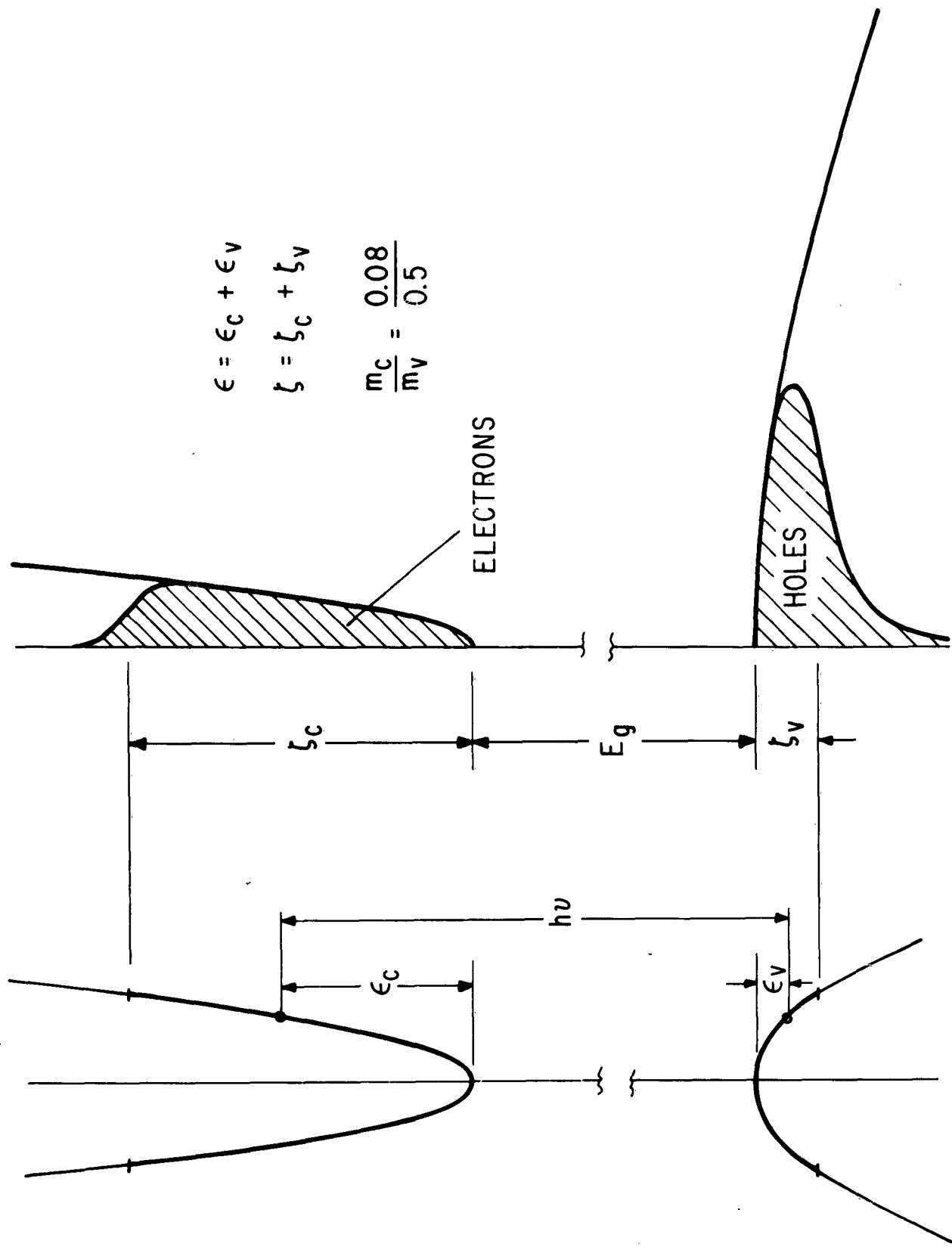
REFERENCES

1. G. J. Lasher, IBM Journal 7, 58 (1963).
2. A. L. McWhorter, H. J. Zeiger, and B. Lax, J. Appl. Phys. 34, 234 (1963).
3. R. N. Hall and D. Olechna, to be published.

FIGURE CAPTIONS

- Fig. 1** Energy vs wave number and energy vs density of states for GaAs, omitting light mass valence band.
- Fig. 2** Threshold current density, junction thickness, and Fermi energy for a GaAs laser, calculated from Eq. 3-6.

FIG. I



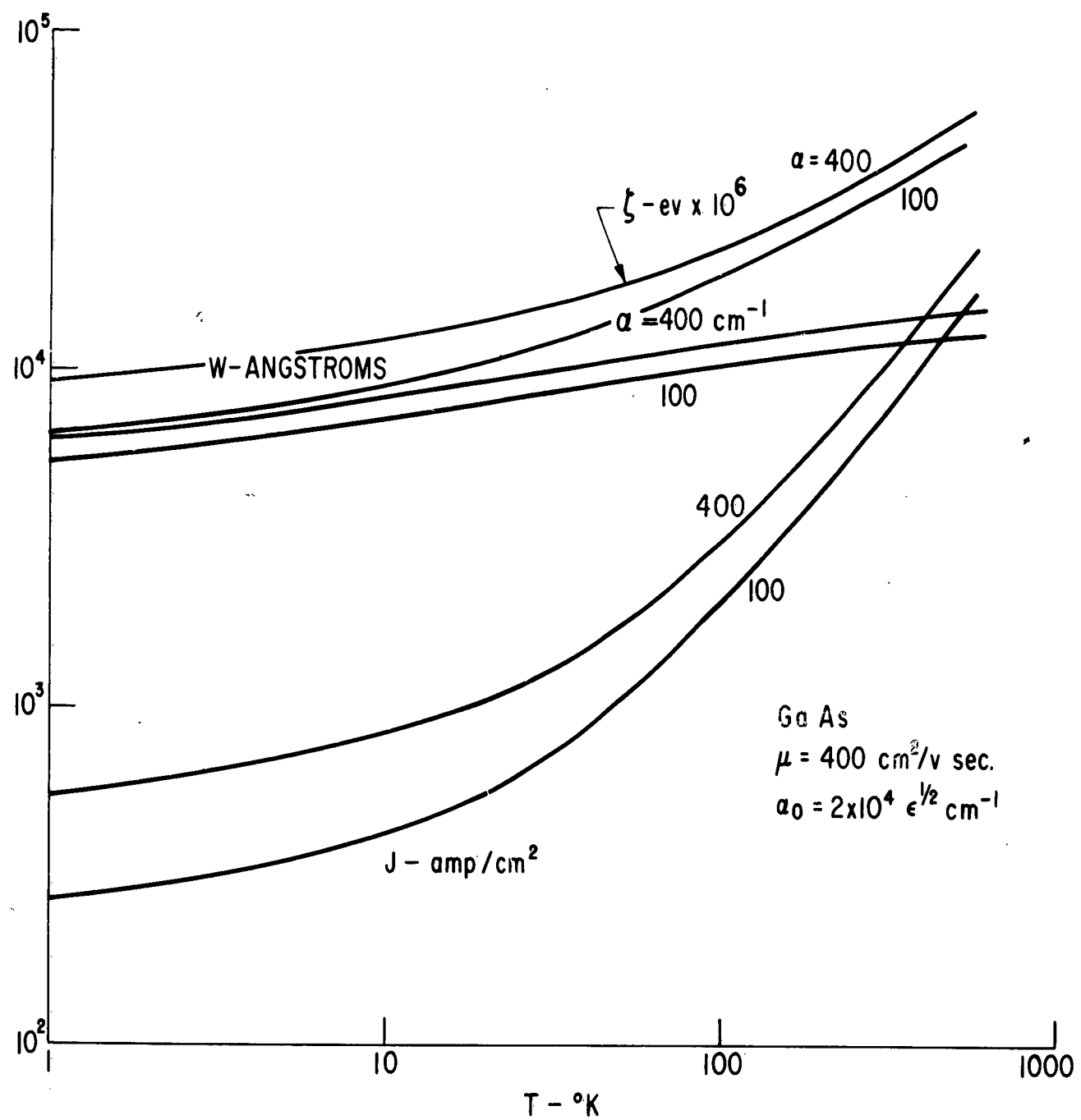


FIG. 2

CONTRIBUTORS

Scientists and technicians who contributed to the work reported:

Staff Members

M Aven
RN Hall
JH Racette
HH Woodbury

Technicians

W Garwacki
B Binkowski
S Schwarz

PAPERS SPONSORED UNDER CONTRACT

M. Lorenz and H. H. Woodbury, Phys. Rev. Letters 10, 215 (1963).

H. H. Woodbury, J. Phys. Chem. Solids, to be published.

B. Segall and M. Aven, Bull. Am. Phys. Soc. 8, 53 (1963).

The following paper gave acknowledgment to supporting work performed under this contract.

J.D. Kingsley and G.E. Fenner, "Stimulated Emission from p-n Junctions," Proceedings of the 3rd International Symposium on Quantum Electronics, Paris (1963).

RNH:erm
4/2/63

